

in each instance) less than that in EOAD for both FTDP-17 (8.5% and 10.0% respectively) and sporadic FTLD with Pick bodies (16.1% and 10.0% respectively). With AT100, the amount of tau detected in FTDP-17 was 54% ($P < 0.001$) of that detected in EOAD, but no tau was detected in sporadic FTLD with Pick bodies using this particular antibody. The amount of insoluble tau deposited within the brain in FTDP-17 did not depend in any systematic way upon where the *MAPT* mutation was topographically located within the gene, or on the physiological or structural change generated by the muta-

tion, regardless of which anti-tau antibody was used. Not only does the amount of tau deposited in the brain differ between the three disorders, but the pattern of phosphorylation of tau also varies according to disease. These findings raise important questions relating to the role of aggregated tau in neurodegeneration – whether this represents an adaptive response which promotes the survival of neurones, or whether it is a detrimental change that directly, or indirectly, brings about the demise of the affected cell.

Keywords: Tau protein, Tau gene, Alzheimer's disease, frontotemporal lobar degeneration, neurofibrillary tangle, Pick bodies

Introduction

Frontotemporal lobar degeneration (FTLD) is a descriptive term given to a clinically and pathologically heterogeneous group of early onset, non-Alzheimer forms of dementia. A previous family history of a similar disorder occurs in about half of patients, and a consensus conference in 1997 highlighted the observations that many such families were linked to a locus on chromosome 17, following which the term frontotemporal dementia with Parkinsonism linked to chromosome 17 (FTDP-17) was derived [1]. In 1998, the disorder was shown [2–4], in certain of these chromosome 17-linked families, to be associated with mutational events in the *tau* gene (*MAPT*), located on the long arm of chromosome 17 (17q21–22). The prevalence of *MAPT* mutations within patients with FTLD varies from about 6–18% [5–7].

To date, more than 35 *MAPT* mutations in over 150 families have been identified, and there is much clinical as well as pathological heterogeneity among the various mutations (see [8,9] for reviews). Some *MAPT* mutations exist as missense mutations within coding regions of exons 1, 9, 11, 12 and 13 [2,3,6,10–19]. Generally, cases with these mutations show swollen nerve cells, and rounded intraneuronal inclusions, reminiscent of the Pick bodies typically seen in some cases of sporadic FTLD, mainly within large and small pyramidal neurones of the cerebral cortex and pyramidal and granule cells of the hippocampus [10–19]. These mutations affect all six isoforms of tau and generate mutated tau molecules that (variably) lose their ability to interact with microtubules, thereby interfering with the promotion of microtubule assembly

and axonal transport [2,3,6,10–20]. Some of the mutations also increase, but again variably, the propensity of the mutated tau to self-aggregate into fibrils that form the characterizing pathological structures within the brain [14–16,18–20].

Other *MAPT* mutations lie close to the splice donor site of the intron that follows the alternatively spliced exon 10 [2–4,6,20–35]. Such cases typically show insoluble aggregated tau deposits as neurofibrillary tangle (NFT)-like structures within large and smaller pyramidal cells of cortical layers III and V, and prominently within glial cells in the deep white matter, globus pallidus and internal capsule [2,3,27,30–34,36,37]. This group of mutations cluster around, or lie within a predicted regulatory stem loop structure of a splice acceptor domain of *MAPT* that determines the inclusion or exclusion of exon 10 by alternative splicing during gene transcription. Such mutations may destabilize this stem loop, and disrupt its function, interfering with the binding of U1snRNP splice regulatory elements, increasing the proportion of tau mRNA transcripts containing exon 10, and the amount of 4-repeat (4R) tau, relative to 3-repeat (3R) tau, protein [2,3]. Other mutations within exon 10 interfere with the splicing ratio between 3R and 4R tau either by strengthening [22,26,35] or destroying [26] the function of splicing-enhancing elements, or by disrupting the function of a splice-silencing element [26,31], in the 5' region of exon 10. Exon 10 mutations like P301L do not affect the splicing of exon 10 [2,26] but induce conformational changes in tau molecules containing exon 10 that interfere with microtubule function, and lead to a specific aggregation of the mutant 4R tau into fibrils [31,35].

Surveys of the published literature infer that not only the distribution and morphology of the insoluble tau aggregate vary greatly in patients with FTLD with *MAPT* mutations according to mutation site and type, but also the total amount of deposited tau can differ. Microscopic observation of cases of FTDP-17 with those of younger individuals with early onset Alzheimer's disease (EOAD) suggests a lower burden of tau pathology. Such observations are somewhat curious and paradoxical given the prevailing view that *MAPT* mutations are the root cause of clinical disability in FTDP-17, whereas in Alzheimer's disease (AD) tau pathology is considered to be a more downstream (to amyloid pathology) event. They also challenge the hypothesis that the accumulation of tau within nerve cells is detrimental to the health of the cell and responsible for its demise.

In the present study we have therefore measured, by image analysis of tau-immunostained sections, and compared the amount of insoluble tau proteins (tau load) in the brains of patients with FTDP-17 with 12 different *MAPT* mutations, patients with sporadic FTLD with Pick bodies and other patients with EOAD.

Materials and methods

Brain tissues were available at autopsy from 34 cases of FTDP-17 with 12 different *MAPT* mutations. Six cases (cases #19–24), one with *MAPT* exon 10 +13 mutation (case #19), and five with *MAPT* exon 10 +16 mutation (cases #20–24) were obtained from the Manchester Brain Bank [37], whereas tissue samples from the other 28 FTDP-17 cases were kindly supplied in collaboration by colleagues from different centres across the world. Selected clinical and pathological details for all cases are given in Table 1. Full clinical and pathological descriptions for 31 of the 34 cases of FTDP-17 have been previously reported by the originating authors (see Table 1 for details of citation); the other three cases remain unreported to date. The 34 FTDP-17 cases (18 men and 16 women) (see Table 1) had mean age of onset of disease of 48.5 ± 7.8 years, range 32–65 years with mean age of death was 57.3 ± 10.0 years, range 38–78 years. The mean disease duration was 8.5 ± 5.5 years, range 2–27. Twelve cases had *APOE* $\epsilon 3/\epsilon 3$ genotype, seven had $\epsilon 3/\epsilon 4$ genotype, five had $\epsilon 2/\epsilon 3$ genotype and one was $\epsilon 2/\epsilon 2$. Only in cases #19 and 20 were there any additional AD-type changes, and then only in the form of some diffuse

amyloid plaques. Neither case had sufficient AD-type pathology to warrant (additional) diagnosis of AD under Consortium to Establish a Registry for Alzheimer's Disease (CERAD) criteria [38]. Braak staging (for AD) [39] was inappropriate.

Tissues were also obtained from 11 cases of sporadic FTLD (cases #35–45) from the Manchester Brain Bank collection, in whom previous pathological investigations [37 and unpublished Mann *et al.*] had shown Pick bodies to be present in the cerebral cortex and hippocampus. Pick bodies were identified, as defined by Kertesz *et al.* [40], as round or oval, compact intracytoplasmic neuronal inclusions, stained by Bielschowsky but not by Galylas, tau-immunoreactive and located in dentate fascia, hippocampus and cerebral cortex. The 11 cases (six men and five women) had a mean age of onset of disease of 57.6 ± 10.4 years, range 46–76 years and mean age of death 66.5 ± 9.2 years, range 56–84 years. The mean disease duration was 8.9 ± 2.7 years, range 4–14 years. Five patients had *APOE* $\epsilon 3/\epsilon 3$ genotype, two had $\epsilon 3/\epsilon 4$ genotype, two had $\epsilon 2/\epsilon 3$ genotype and one was $\epsilon 2/\epsilon 2$. None of these cases showed any coincidental AD-type pathology.

All 25 cases of EOAD (11 men and 14 women) were from the Manchester Brain Bank collection. These had a mean age of onset of disease of 53.4 ± 6.6 years, range 35–60 years and mean age of death 62.9 ± 8.0 years, range 44–73 years. The mean disease duration was 9.5 ± 3.5 years, range 4–19 years. Sixteen patients had *APOE* $\epsilon 3/\epsilon 3$ genotype, seven had $\epsilon 3/\epsilon 4$ genotype, one had $\epsilon 2/\epsilon 3$ genotype and one had $\epsilon 2/\epsilon 2$ genotype. All cases were consistent with CERAD pathological criteria for AD [38], and all were at Braak stages 5 or 6 [39]. In none of the cases was there a previous family history of disease consistent with autosomal dominant inheritance.

We chose not to include a control group of nondemented persons within the study because the primary purpose was to investigate how the level of tau deposition in FTLD compared with that in EOAD. Moreover, the great majority of cases studied, FTLD or AD, were less than 65 years of age at death, and it is uncommon for significant tau pathology to be present in normal individuals in that age range. Furthermore, although cases of corticobasal degeneration (CBD) and progressive supranuclear palsy (PSP) are subsumed under some pathological criteria for FTLD [41], we did not include such cases in this present study. This was because in CBD, tau pathology is within glial cells as well as neurones, and principally affects parietal cortex rather than frontal lobes, whereas

Table 1. Selected clinical and pathological details of cases investigated

Case	Diagnosis	MA1P mutation	Gender	Age at onset (year)	Age at death (year)	Duration (year)	APOE genotype	Brain weight (g)
1 [18]	FTDP-17	L266V	M	32	36	3.5	NA	1050
2 [30]	FTDP-17	N279K	M	46	57	11	3.3	1250
3 [30]	FTDP-17	N279K	M	44	50	6	3.3	1420
4 [20]	FTDP-17	N279K	M	44	50	6	3.4	1290
5 [20]	FTDP-17	N279K	F	45	48	3	3.3	1100
6 [20]	FTDP-17	N279K	M	56	58	2	2.3	1400
7 [20]	FTDP-17	N279K	F	45	53	8	2.4	1000
8 [20]	FTDP-17	N279K	M	57	63	6	3.4	1100
9 [20]	FTDP-17	N279K	M	41	52	11	2.3	1100
10 [25]	FTDP-17	N279K	M	40	47	7	NA	1230
11 [33]	FTDP-17	N296H	M	57	62	3	3.3	960
12 [6.21]	FTDP-17	P301L	M	48	60	12	3.3	1331
13 [6.21]	FTDP-17	P301L	F	50	66	15	3.3	856
14 [6.21]	FTDP-17	P301L	M	44	52	8	2.3	1087
15 [6.21]	FTDP-17	P301L	F	54	76	22	2.2	1006
16 [6.21]	FTDP-17	P301L	F	59	64	5	3.3	1013
17 [28]	FTDP-17	P301L	F	48	55	7	NA	915
18 [32,36]	FTDP-17	S305S	F	48	51	3	NA	1053
19 [2.34]	FTDP-17	Exon 10 +13	M	65	70	5	3.4	1100
20 [2.34]	FTDP-17	Exon 10 +16	M	50	61	11	3.4	1016
21 [2.34]	FTDP-17	Exon 10 +16	F	46	58	12	3.3	996
22 [2.34]	FTDP-17	Exon 10 +16	M	43	55	12	3.4	1240
23 [34]	FTDP-17	Exon 10 +16	F	52	65	13	2.3	1040
24 [34]	FTDP-17	Exon 10 +16	F	48	56	8	3.4	1175
25 [un]	FTDP-17	Exon 10 +16	F	43	52	9	2.3	1138
26 [19]	FTDP-17	Q336R	M	58	68	10	3.3	1102
27 [12]	FTDP-17	G342V	F	48	55	7	3.3	1020
28 [15]	FTDP-17	K369I	F	52	61	9	NA	885
29 [13]	FTDP-17	G389R	F	32	37	5	3.3	1006
30 [un]	FTDP-17	G389R	M	45	49	4	NA	1170
31 [11]	FTDP-17	G389R	M	38	43	5	NA	NA
32 [6.21]	FTDP-17	R406W	M	63	70	7	3.3	1121
33 [6.21]	FTDP-17	R406W	F	58	71	13	3.4	905
34 [un]	FTDP-17	R406W	F	49	78	29	NA	1035
35 [37]	Pick	None	F	53	60	7	3.3	960
36 [37]	Pick	None	M	46	56	10	3.3	1150
37 [37]	Pick	None	M	NA	NA	NA	NA	NA
38 [37]	Pick	None	F	52	62	10	3.4	928
39 [37]	Pick	None	F	76	84	8	3.3	1235
40 [37]	Pick	None	F	50	58	8	2.2	1065
41 [37]	Pick	None	M	63	74	11	2.3	990
42 [37]	Pick	None	M	73	77	4	3.3	NA
43 [37]	Pick	None	F	57	64	7	3.3	1000
44 [37]	Pick	None	M	47	61	14	3.4	980
45 [un]	Pick	None	M	59	69	10	2.3	NA
46	AD	None	F	54	59	5	3.3	1008
47	AD	None	F	56	62	6	3.3	1020
48	AD	None	M	55	60	5	3.4	1368
49	AD	None	F	57	67	10	3.4	1018
50	AD	None	F	39	45	6	3.3	NA
51	AD	None	M	40	44	4	3.3	1400
52	AD	None	F	52	71	19	3.3	910
53	AD	None	M	35	45	10	3.4	1177

Table 1. *Continued*

Case	Diagnosis	MAPT mutation	Gender	Age at onset (year)	Age at death (year)	Duration (year)	APOE genotype	Brain weight (g)
55	AD	None	F	58	70	12	3.4	1026
56	AD	None	F	52	61	9	3.3	906
57	AD	None	F	52	64	12	2.2	1120
58	AD	None	F	54	67	13	3.3	947
59	AD	None	M	55	61	6	3.3	NA
60	AD	None	M	60	72	12	3.4	1251
61	AD	None	F	60	73	13	3.3	1028
62	AD	None	F	52	61	9	3.3	1262
63	AD	None	M	56	66	10	3.3	1070
64	AD	None	F	59	71	12	3.3	1208
65	AD	None	M	55	64	9	2.3	1275
66	AD	None	F	48	60	12	3.4	1050
67	AD	None	M	59	64	5	3.3	1330
68	AD	None	M	57	67	10	3.3	1158
69	AD	None	M	60	66	6	3.3	1206
70	AD	None	M	58	70	12	3.4	1314

FTDP-17, frontotemporal dementia with Parkinsonism linked to chromosome 17; Pick, frontotemporal lobar degeneration with Pick bodies; AD, Alzheimer's disease; un, unpublished case. NA, no details available. Citation numbers in parentheses.

in PSP, tau pathology is mostly within neurones and glial cells in subcortical structures. Therefore, although such disorders can likewise be considered as tauopathies, measurement of tau load within frontal cortex was not considered to be informative, at least as regards the purpose of the present investigation.

Serial sections from formalin-fixed, wax-embedded blocks of frontal cortex (BA 8/9) were cut at a thickness of 6 µm and mounted on 3-aminopropyltriethoxysilane (APES)-coated slides. Sections were immunostained for insoluble tau proteins by a standard immunoperoxidase method [37], using the phospho-dependent tau antibodies AT8 (1:750 dilution), AT100 (1:200 dilution) and AT180 (1:200 dilution) (all from Innogenetics, Belgium). AT8 antibody is raised against phosphorylated Ser202 epitope and immunoreacts with paired helical filament (PHF) tau in AD [42]. AT100 antibody is raised against phosphorylated Thr212/Ser214 epitopes and labels only pathological tau [43]. AT180 antibody is raised against phosphorylated Thr231 epitope, and labels approximately 70% of PHF in AD brain, but also labels phosphorylated foetal and adult normal tau [44].

The amount of insoluble tau (tau load) within AT8-, AT100- and AT180-immunostained sections was quantified by Image Analysis. The system employed uses Leica Image Analysis software and a Leica Microscope with Quantimet 570 Image Analyser. Measurement of tau load

was performed only on grey matter regions. The area for measurement, which extended from the surface of the cortex to the grey/white matter boundary, was identified under the microscope at ×5 magnification. After optimizing the computer captured image for colour and staining density, the total measured area and area of tissue occupied by stained product were determined using in-house software. The software employed allows the segmented image to be directly overlaid upon the captured image so that with optimal thresholding it can be ensured that all tau-immunostained stained objects (for example, NFT, neuropil threads and plaque neurites in AD, NFT or Pick bodies in FTL and FTDP-17) are recognized. To ensure comparability between cases, the particular area measured was systematically sampled so that the measured field was always on a 'straight' section of the cortex, away from the depths or the crown of the gyrus, and away from 'bad quality tissue' (that is, tissue areas containing artefactual staining or splits or tears in the section). The total area of cortex measured in each field averaged 1.43 mm². Tau load was calculated as the percentage of total area occupied by immunostained product. Trial measurements, employing cumulative mean statistic, were initially performed to determine the number of fields required to be measured for the mean to fall within 95% confidence levels for each antibody. In this way it was determined that for AT8-immunostained sections six measurements were

necessary, and for AT100- and AT180-immunostained sections four measurements were required. The mean tau load was calculated for each section.

Image Analysis data was analysed using the Statsdirect statistical package. Because the mean tau load data obtained from AT8-immunostained sections did not follow a normal distribution, logarithmic transformation was performed. A one way analysis of variance test (ANOVA) was then used to compare differences in tau deposition between each disease group with *post hoc* unpaired *t*-tests being performed where results of ANOVA were significant. The tau load data obtained for sections stained with AT100 and AT180 likewise did not follow a normal distribution, even when logarithmically transformed. Therefore, Kruskal-Wallis test was used to compare differences in tau deposition between each disease group with *post hoc* Mann-Whitney *U*-tests being performed when result of Kruskal-Wallis was significant. Comparison of tau load between bearers and non-bearers of *APOE* $\epsilon 4$ allele in each disease group were performed for all antibodies using Mann-Whitney *U*-test. For all statistical tests a *P*-value less than 0.05 was considered significant.

In order to investigate the effect of different *MAPT* mutations on tau load, the cases were categorized into four groups according to mutation type:

Group A – cases ($n = 18$) with *MAPT* mutations which affect splicing of exon 10 increasing the 4R : 3R ratio of tau isoforms and producing mostly NFT pathology (mutations: N279K, N296H, S305S, +16, +13).

Group B – cases ($n = 16$) with *MAPT* mutations which alter the tau protein and have been shown to affect microtubule binding (mutations: L266V, Q336R, G342V, K369I, G389R, P301L, R406W).

Group C – cases ($n = 7$) with *MAPT* mutations which alter the tau protein and have been shown to affect microtubule binding, but produce only Pick-type pathology (mutations: L266V, Q336R, G342V, K369I, G389R).

Group D – cases ($n = 9$) with *MAPT* mutations which alter the microtubule binding of the protein, but do not affect exon 10 splicing, and produce mostly NFT-type pathology (mutations: P301L, R406W).

Mann-Whitney *U*-tests were performed between these groups to investigate differences in tau deposition between different groups of *MAPT* mutations. Mann-Whitney *U*-test was also performed to investigate differences in tau deposition between FTDP-17 group C cases with Pick-type bodies and sporadic FTLD cases with Pick bodies. Mann-Whitney *U*-tests were also performed to assess differences

in relative immunoreactivity between AT8, AT100 and AT180 antibodies, for each disease group. Spearman rank correlation test was used to determine correlations between tau load and duration and age of onset of disease in each disease group.

Results

Morphological descriptions of tau pathology, using the present, or other similar, tau antibodies, on those FTDP-17 patients studied here have been fully reported previously by both ourselves [13, 19, 34, 37] and other workers [6, 10–12, 15, 18, 25, 28, 30, 32–34, 36], as have those patients with sporadic FTLD with Pick bodies from our own series of FTLD cases [37], and such observations are therefore not repeated in this present study. Likewise, the immunohistochemical pattern of tau pathology in the AD cases was entirely typical of the disorder, and is likewise not described further in this report.

Comparison of tau load between the three disease groups

Mean tau load detected for each disease group, for each antibody, is shown in Table 2. For AT8 antibody, there was a highly significant difference in tau load between the three disease groups ($F_{2,31} = 44.4$; $P < 0.0001$) so that mean tau load in FTDP-17, and in sporadic FTLD with Pick bodies, were both significantly less ($P < 0.001$) than that in EOAD. There was a trend ($P = 0.057$) towards

Table 2. Mean (\pm SD) tau load in frontal cortex as detected by phospho-dependent antibodies AT8, AT100 and AT180 in 34 patients with FTDP-17, 11 with sporadic FTLD with Pick bodies and 25 with EOAD

	AT8	AT100	AT180
FTDP-17	1.2 \pm 1.1	1.5 \pm 1.5	0.9 \pm 0.8
<i>MAPT</i> mutation Group A	1.1 \pm 1.2	1.1 \pm 1.5	0.7 \pm 0.9
<i>MAPT</i> mutation Group B	1.4 \pm 1.0	2.0 \pm 1.4	1.0 \pm 0.6
<i>MAPT</i> mutation Group C	1.7 \pm 1.2	1.6 \pm 1.5	0.8 \pm 0.5
<i>MAPT</i> mutation Group D	1.1 \pm 0.8	2.2 \pm 1.3	1.2 \pm 0.7
Sporadic FTLD with Pick bodies	2.3 \pm 1.5	0 \pm 0	0.9 \pm 0.6
EOAD	14.3 \pm 12.8	2.8 \pm 3.1	9.0 \pm 11.0

FTDP-17, frontotemporal dementia with Parkinsonism linked to chromosome 17; FTLD, frontotemporal lobar degeneration; EOAD, early onset Alzheimer's disease.

mean tau load in FTDP-17 being less than that in sporadic FTLD with Pick bodies.

For AT180 antibody, using Kruskal–Wallis test, there was a highly significant difference in mean tau load between the three disease groups ($\chi^2 = 27.9$; $P < 0.0001$) so that mean tau load in FTDP-17, and in sporadic FTLD with Pick bodies, was significantly less ($P < 0.001$) than that in EOAD. There was no significant difference ($P = 0.918$) in mean tau load between FTDP-17 and sporadic FTLD with Pick bodies.

For AT100 antibody (again using Kruskal–Wallis test) there was also a highly significant difference in mean tau load between the three disease groups ($\chi^2 = 24.5$; $P < 0.0001$). Indeed, there was little or no (measurable) staining of Pick bodies with AT100. Mean tau load in FTDP-17, and in EOAD, was consequently greater

($P < 0.001$) than that in sporadic FTLD with Pick bodies. Mean tau load in FTDP-17 was less (but not significantly so, $P = 0.083$) than that in patients with EOAD.

Differences in tau deposition within the FTDP-17 group

The extent of tau deposition was compared in FTDP-17 according to *MAPT* mutation position or type. When plotted against the topographical position of the *MAPT* mutation (coding for the longest tau isoform), no clear cut individual differential effect of any of the *MAPT* mutations on the extent of tau deposition within the frontal cortex was seen, either for AT8, AT100 or AT180 antibodies (Figure 1). Nonetheless, with AT8 immunostaining, *MAPT* L266V and exon 10 +13 splice mutation showed

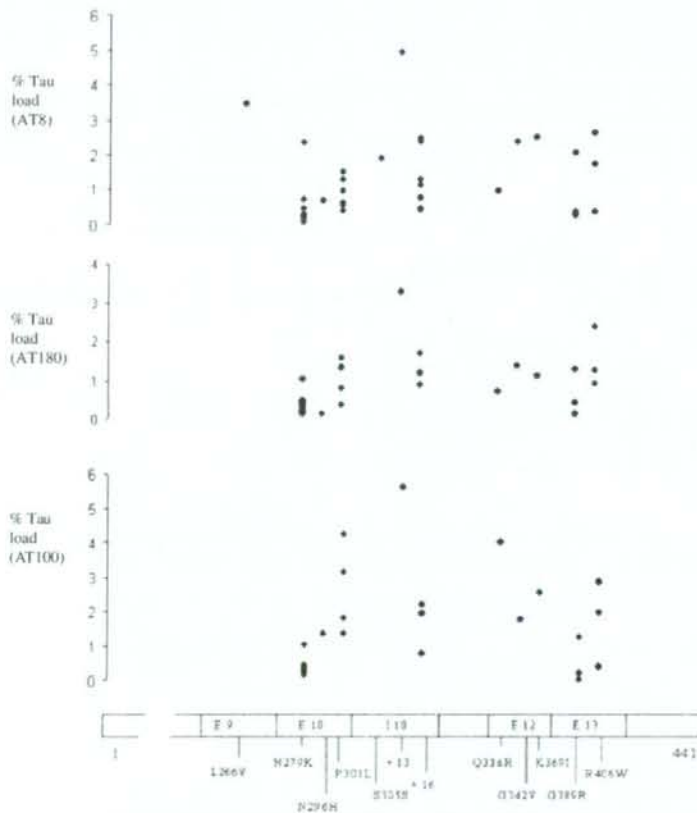


Figure 1. Tau load detected in each case for each of the mutations; E indicates exons on the gene; I indicates intron.

particularly heavy tau deposition, relative to the other cases. For L266V, this is consistent with the involvement of all the cortical layers of grey matter and some astrocytic staining in the pathological process (see also [18]). In the exon 10 +13 mutation, this could be explained by the presence of many tau-positive neuritic plaques in the superficial layers of the cortex (see also [34]). For AT180, again as explained, exon 10 +13 splice mutation showed particularly heavy tau deposition. However, for AT100 some of P301L cases, and the Q336R case, were heavily stained relative to AT8 and AT100 (Figure 1).

As detailed in *Methods* section, the mutation cases were grouped in order to investigate the effect of different *MAPT* mutation types on tau load. No significant differences in mean tau load were seen between any of the four *MAPT* mutation groups as detected by either AT8 ($\chi^2 = 1.05$; $P = 0.789$), AT180 ($\chi^2 = 2.86$; $P = 0.413$) or AT100 ($\chi^2 = 6.52$; $P = 0.09$) antibodies (Table 2). The mean tau load in FTDP-17 cases with Pick-type bodies (that is, Group C cases) did not differ from that seen in sporadic FTLD with Pick bodies for either AT8 ($P = 0.375$) or AT180 antibodies ($P = 0.887$) (Table 2), although interestingly AT100 immunostained Pick bodies in Group C cases (cf lack of Pick body staining in sporadic FTLD with Pick bodies).

Comparisons of relative immunoreactivities of each antibody

In general, in FTDP-17, AT8 and AT100 gave similar degree of immunostaining, whereas AT180 antibody showed less immunoreactivity (Table 2), although for some *MAPT* mutations (for example, R406W, N279K, exon 10 +16, G389R mutations) the tau load detected by

AT8 and AT180 antibodies was similar. Again, in general, AT100 antibody showed slightly more immunoreactivity than AT8, but in some instances AT8 and AT100 immunoreactivity was the same (for example, K369I, G342V, exon 10 +13 mutations) and for some (for example, P301L mutation) AT100 gave stronger staining than AT8. However, statistically, the mean tau load detected by AT8, AT100 or AT180 antibodies did not vary significantly ($\chi^2 = 2.1$; $P = 0.340$) (Table 2).

In sporadic FTLD with Pick bodies, and EOAD, mean tau load detected by each antibody varied significantly ($\chi^2 = 24.8$ and $\chi^2 = 22.4$ respectively; $P < 0.0001$ for both). *Post hoc* testing showed that in both of these disease groups, mean tau load detected by AT8 was greater than that detected by either AT100 ($P < 0.0001$ in both instances) or AT180 ($P = 0.004$ and $P = 0.026$ respectively), and that mean tau load detected by AT180 was greater than that detected by AT100 in both disease groups ($P < 0.0001$ in both instances).

Effect of possession of the APOE $\epsilon 4$ allele

Mean percentage tau load, as detected by AT8, AT100 or AT180 antibodies, in patients with *APOE* $\epsilon 4$ allele was not significantly different from that detected in those without *APOE* $\epsilon 4$ allele for any of the three disorders (Table 3)

Correlations with age of onset of disease and duration of illness

With AT8, no significant correlation between duration of illness and tau load was found for any of the three disorders ($r_s = 0.07-0.09$; $P = 0.595-0.838$). For the age of onset of disease no significant correlations were found

Table 3. Mean (\pm SD) tau load in frontal cortex as detected by phospho-dependent antibodies AT8, AT100 and AT180 in 34 patients with FTDP-17, 11 with sporadic FTLD with Pick bodies and 25 with EOAD, stratified into those bearing *APOE* $\epsilon 4$ allele and those without *APOE* $\epsilon 4$ allele

	<i>APOE</i> status	AT8	AT100	AT180
FTDP-17	With $\epsilon 4$ allele	1.7 \pm 1.7	1.5 \pm 1.6	1.2 \pm 1.3
	Without $\epsilon 4$ allele	0.9 \pm 0.7	1.9 \pm 2.1	0.8 \pm 0.6
Sporadic FTLD with Pick bodies	With $\epsilon 4$ allele	2.3 \pm 1.5	0 \pm 0	0.7 \pm 0.8
	Without $\epsilon 4$ allele	2.3 \pm 0.3	0 \pm 0	1.0 \pm 0.7
EOAD	With $\epsilon 4$ allele	15.0 \pm 12.5	2.9 \pm 3.3	12.5 \pm 13.0
	Without $\epsilon 4$ allele	13.5 \pm 12.5	2.8 \pm 3.2	7.6 \pm 10.3

FTDP-17, frontotemporal dementia with Parkinsonism linked to chromosome 17; FTLD, frontotemporal lobar degeneration; EOAD, early onset Alzheimer's disease.

with tau load for either FTDP-17 ($r_s = 0.09$; $P = 0.623$) or EOAD ($r_s = 0.37$; $P = 0.070$), but a significant inverse correlation was found in sporadic FTL with Pick bodies ($r_s = -0.850$; $P = 0.002$). Similar findings were seen with AT100 and AT180 (data not shown).

Discussion

The effect of 12 different mutations in *MAPT* on the amount of tau protein deposited in the brain has been investigated in this study using immunohistochemical staining with three phosphorylation-dependent anti-tau antibodies. We grouped the mutations according to their functional effects, or pathological characteristics, looking for differences in effect between those mutations (Group A) which affect splicing of exon 10 increasing the 4R : 3R ratio of tau isoforms and produce mostly NFT pathology with those missense mutations outside exon 10 (Group B) that change the protein structure of tau and affect all tau isoforms and interfere with microtubule binding. We also compared mutations that generate a Pick body-like pathology (Group C) with those that alter the microtubule-binding capability of tau, but do not affect exon 10 splicing and produce mostly NFT-type pathology (Group D). In no instance did we find any significant group differences in the extent of tau deposition with any of the antibodies, nor did any single mutation appear to have any preferential effect in this respect, although singleton cases of L266V and exon 10 +13 splice mutation did show relative (to other mutations) high tau loads with AT8 and AT180. In the former case there were unusually high levels of tau within grey matter astrocytes [see, also 18], while in the latter case there was a heavy tau burden within neuritic plaques [see 34], in accordance with age and possession of APOE $\epsilon 4$ allele [45]. Some P301L cases and the single Q336R case showed disproportionately (relative to AT8 and AT180) high tau loads with AT100. Hence, we find that the amount of tau deposited in the brain in FTDP-17 does not seem to be determined either by topographic position within *MAPT*, or the physiological change in tau function induced by such a mutation. Neither does the isoform composition of the aggregated tau seem to influence the amount of tau deposited because there was no difference in tau load between Group B cases, which lead to a tau deposition with a mix of (mostly) 3R and 4R tau isoforms [see 10–13, 15, 18, 19], and Group A cases, where the tau protein is known to be mostly, or only, 4R [see 22, 25, 28, 30–34, 36]. This implies that both types

of mutation, despite having a different primary effect on the tau protein itself, ultimately affect cellular function (possibly microtubule stability) in a similar way and/or to a similar degree. Similarly, the amount of tau deposited in the form of Pick bodies in FTDP-17 is not different from that seen in cases of sporadic FTL characterized by Pick body formation.

Interestingly, and perhaps paradoxically, the amount of tau deposited in FTDP-17 or in FTL with Pick bodies, irrespective of the physiological change in tau invoked (that is, mutational or posttranslational respectively), as detected by AT8 and AT180 antibodies, was about one-tenth of that deposited in EOAD. Because the cases were matched for age at onset and duration of disease, it is unlikely that these differences in tau load reflect demographic variations or differences in stage of the disease at death. Indeed, there were no correlations between tau load and duration of illness for any of the disease groups. However, because, in AD at least [46, 47], tau proteins are incorporated into aggregated filamentous structures on a whole molecule basis, and not as a series of (variably) truncated molecules, it might be argued that variations in tau load between disorders using these two antibodies reflect differences in degree of phosphorylation of tau at different epitopes, or ease of antibody accessibility, rather than actual number of tau molecules present. These considerations are unlikely to explain the very high differences in tau load between FTL and EOAD with AT8 antibody at least, because biochemical measures of insoluble tau load by Western blot using this particular antibody have also shown much greater quantities of insoluble tau within the brain in AD compared with FTL cases (Hasegawa, unpub. data). Present data suggest therefore that there is a lower accumulation of pathological tau over the span of the illness in the brains of patients with FTL, irrespective of underlying cause, compared with those with AD. The reason for this lower tissue accumulation of tau lies mostly with differing anatomical compartmentalization. In AD the pathological tau deposits are present within neuronal cell bodies (as NFT), dendrites (as neuropil threads) and in axon terminals in neuritic plaques. Tau load in AD, as measured here, represents the composite total of these three anatomical compartments. However, in FTDP-17, and in FTL with Pick bodies, the bulk of the pathological tau is perikaryal, with little neuropil staining in most instances, except as above where there may be additional glial tau or neuritic plaques present.

The results obtained with AT100 antibody are interesting. AT100 labels pathological aggregations of the PHF in NFT in AD, but does not label normal tau [43]. This antibody detects phosphorylated epitopes Thr212/Ser214 in PHF with the epitope being achieved by the sequential phosphorylation of tau at Thr212 by GSK-3 β , then at Ser214 by protein kinase A (PKA) in the presence of polyanions such as heparin and tRNA [48]. In this present study, there was little or no immunoreactivity with AT100 in cases of FTLD with Pick bodies, in contrast to cases of AD and FTDP-17. This suggests that in FTLD with Pick bodies either the requirements needed for the formation of the AT100 epitope [48] are not fulfilled, and the epitope is therefore not phosphorylated, or that the tertiary structure of tau in Pick bodies upon fixation makes the epitope inaccessible even though it may be phosphorylated. Maillot and co-workers [49] have detected, by Western blot, insoluble tau in brain tissue of cases of FTLD with Pick bodies using AT100, implying that this epitope is indeed phosphorylated, and that changes in the conformational structure of Pick bodies on tissue fixation may be masking the AT100 epitope. This is quite possible, because low or no Pick body immunoreactivity has been observed with another phosphorylation-dependent antibody, 12E8, raised against the Ser262 epitope [37,50]. However, in this instance, it was also not possible, using 12E8, to detect tau proteins from FTLD cases with Pick bodies on Western blotting [49], implying that a non-phosphorylation of this particular epitope is responsible for the lack of detection of tau in Pick bodies. In AD [51] and MAPT exon 10 +16 [34,37] cases, 12E8 specifically stains well-formed NFT rather than pretangles; AT100, likewise, stains NFT strongly, and pretangles less strongly [43]. Nonetheless, in another study, Ferrer and colleagues used a different (to 12E8) antibody against Ser262 epitope (Ser²⁶²), which in AD stains pretangles, and showed Pick bodies to be strongly reactive [52]. Hence, the reason for the lack of Pick body staining with AT100 is still not clear.

Also of particular note are findings in MAPT P301L mutation where AT100 antibody stained tau aggregations much more strongly than the other two antibodies, in contrast to other MAPT mutations where AT8 was usually strongest (see Figure 1). It is therefore possible that protein conformational changes induced by this mutation may help to fulfil the requirements for formation of the Thr212/Ser214 epitope [48]. However, the Ser202 (AT8) epitope needs to be phosphorylated before formation of the

AT100 epitope [48], yet in P301L mutation AT8 immunoreactivity was less than that of AT100. This suggests that conformational changes of tau protein, potentially induced by P301L mutation, confer a lesser accessibility of the AT8 antibody to its epitope, which although phosphorylated is relatively undetected, while in contrast such changes enhance the detection of the AT100 Thr212/Ser214 epitope.

On face value, present findings might therefore suggest that FTLD is a pathologically 'less aggressive' illness than AD. Because there is greater tissue loss in FTLD than in AD, it might be argued that the accumulation of aggregated tau proteins within neurones in FTLD is incidental and epiphenomenal to the main disease process that leads to the gross neurodegeneration seen in these cases. However, it may also be the case that MAPT mutations cause changes in cellular function so lethal to the nerve cell that death occurs before (many of) the cells can accumulate (much) tau. One direct effect of the MAPT missense mutations leads to formation of mutated tau molecules that lose ability to bind microtubules and reduce microtubule assembly resulting in impaired axonal transport [22]. Exon 10 mutations increase the ratio between 4R : 3R tau and perturb the precisely regulated stoichiometric binding of tau proteins to tubulin needed for microtubule assembly [53]. Hence, catastrophic disruption in protein transport leading to cell death may occur in many neurones without significant tau accumulation having taken place.

It has been shown that unpolymerized hyperphosphorylated tau proteins in the cell cytosol can sequester normal functional tau, forming filaments and leading to inhibition and disassembly of microtubules [54]. However, polymerized tau in the form of PHF does not possess this ability [55]. In AD, neurones may therefore 'promote' PHF formation from hyperphosphorylated tau in order to protect normal cytosolic tau from being sequestered into filaments, thereby allowing cells to survive longer [56]. Because tau in AD is neither mutated nor produced in a stoichiometrically unbalanced way, it is possible therefore that microtubule formation and function can be maintained (longer than in FTLD) despite the accumulation of PHF. Tau aggregation may therefore be a protective or an adaptive response of neurones. Due to the catastrophic effect of MAPT mutations on microtubule function, this process in FTLD is inefficient or ineffective, and many nerve cells die without ever accumulating (much) tau. Only those (relatively few) nerve cells better able to resist

the cellular effects of the mutation, and to 'package' abnormal tau molecules into aggregates, are able to function for longer. However, even in AD, accumulation of tau as PHF is not without detriment, with progressive loss of endoplasmic reticulum and ribosomes with accumulating PHF [57], indicating a decline in the nerve cell's synthetic machinery that eventually crosses a threshold to continued survival.

In sporadic FTLD with Pick bodies it is presumed that, as in FTDP-17, loss of microtubule function is likewise invoked through post-translational hyperphosphorylation changes in tau, although as yet the precise mechanism underpinning this is not known. Nonetheless, tau deposition is again about 10 times less than that in EOAD and the same mechanistic arguments (as in FTDP-17) for this smaller accumulation of tau may apply.

However, it could also be argued that the lower level of tau accumulated in FTLD compared with AD reflects the relative ease of degradation and clearance in each disorder with more pathological tau being removed from the brain during the course of the illness than is possible in AD. In AD, the hyperphosphorylated tau is assembled into highly insoluble PHF that become heavily modified through processes such as glycation [58]. Certainly, under the electron microscope, tau filaments in FTLD and AD have different ultrastructural appearances. In FTLD, the tau filaments are usually straight (with some twisted filaments) in those *MAPT* mutations in which Pick bodies are present [13], whereas the NFT-like structures in cases with exon 10 and splice mutations are composed of wide flat twisted ribbons [34], not PHF. These latter filamentous types may be more susceptible to degradation both internally and externally than PHF which even after cell death in AD remain largely intact as 'ghost tangles'. However, the lack of excessive tau in R406W mutation (compared with other *MAPT* mutations), where tau is present as PHF [6,21], would argue against this, although the long disease durations present in many patients with this particular mutation (in the three cases studied here disease duration was 7–29 years) suggests an unusually mild pathological phenotype with the low tau levels being a reflection of this. It would be interesting to compare tau loads using antibodies against glycation end-products or anti-tau antibodies like Alz50 and TG-3 which recognize tau only in specific conformations [59].

It might further be argued that even though the frontal cortex contains tau pathology for all three diseases under investigation, this might not be an appropriate or repre-

sentative brain region to work on in a study of this kind, being affected relatively less than other regions (for example, temporal cortex) at end-stage disease at least as far as AD, and maybe also sporadic FTLD with Pick bodies [60] and FTDP-17 cases with N279K (in which a movement disorder is prominent) [20,23] are concerned. However, because the frontal cortex is not 'saturated' by tau pathology, even at end-stage disease, its study should better allow the relationship between tau deposition and *MAPT* mutation, or disease type, to be determined than would be the case were end-stage 'burnt out' regions like temporal cortex to be examined. The low levels of tau in frontal cortex in FTLD compared with those in AD could reflect declining disease in this region in FTLD, and that there could be regions of the brain in this latter disorder where the disease process is evolving more actively. However, histological examination of the brain in FTLD with respect to tau deposition refutes this where the level of tau deposition declines when moving in an anterior-posterior direction into better preserved regions of (frontal and parietal cortex) [13,34].

One potential weakness of the present study is that we have only employed phosphorylation-dependent tau antibodies and therefore the tau measurements we have obtained with any given antibody might reflect, at least partially, that proportion of tau molecules in which the epitope concerned is accordingly phosphorylated. As mentioned earlier in connection with AT100 immunostaining, different levels of phosphorylation at different epitopes on tau, or antibody accessibility, might explain the variations in mean tau load between antibodies, and between disease groups. In order to determine whether the antibodies we have used here have detected all, or only a proportion of, the insoluble tau pathology, it will be necessary to perform further analysis using a phospho-independent antibody, or to compare insoluble tau loads by biochemical techniques.

In conclusion, we suggest that the amount of insoluble tau deposited within the brain in FTLD does not depend in any systematic way upon the presence, or type, of *MAPT* mutation, or on what physiological change is generated. Furthermore, the brain tau load in FTLD would seem to be considerably less than that in EOAD, and this finding raises important questions relating to the role of aggregated tau in neurodegeneration – whether this represents an adaptive response aimed at promoting survival of neurones, or is indeed a detrimental change which brings about the demise of the affected cell.

Acknowledgements

This study was supported by a Wolfson Scholarship to AMS and Alzheimer's Research Trust Alzheimer's Disease Research Centre Grant to DMAM. The authors wish to thank the many other people who were involved in collecting and characterizing the FTLD cases with MAPT mutations, and the other FTLD and EOAD cases, and by doing so making possible this multicentre collaborative study.

References

- Foster NL, Wilhelmsen K, Sima AA, Jones MZ, D'Amato CJ, Gilman S. Frontotemporal dementia and parkinsonism linked to chromosome 17: a consensus conference. *Ann Neurol* 1997; **41**: 706–15
- Hutton M, Lendon CL, Rizzu P, Baker M, Froelich S, Houlden H, Pickering-Brown S, Chakraverty S, Isaacs A, Grover A, Hackett J, Adamson J, Lincoln S, Dickson D, Davies P, Petersen RC, Stevens M, de Graaff E, Wauters E, van Baren J, Hillebrand M, Joosse M, Kwon MJ, Nowotny P, Che LK, Norton J, Morris JC, Reed LA, Trojanowski JQ, Basun H, Lannfelt L, Neystat M, Fahn S, Dark F, Tannenberg T, Dodd PR, Hayward N, Kwok JB, Schofield PR, Andreadis A, Snowden J, Craufurd D, Neary D, Owen F, Oostra BA, Hardy J, Goate A, van Swieten J, Mann D, Lynch T, Heutink P. Association of missense and 5'-splice-site mutations in tau with the inherited dementia FTDP-17. *Nature* 1998; **393**: 702–5
- Poorkaj P, Bird TD, Wijsman E, Nemens E, Garruto RM, Anderson L, Andreadis A, Wiederholt WC, Raskind M, Schellenberg GD. Tau is a candidate gene for chromosome 17 frontotemporal dementia. *Ann Neurol* 1998; **43**: 815–25
- Spillantini MG, Murrell JR, Goedert M, Farlow MR, Klug A, Ghetti B. Mutation in the tau gene in familial multiple system tauopathy with presenile dementia. *Proc Natl Acad Sci USA* 1998; **95**: 7737–41
- Houlden H, Baker M, Adamson J, Grover A, Waring S, Dickson D, Lynch T, Boeve B, Petersen RC, Pickering-Brown S, Neary D, Craufurd D, Snowden JS, Mann D, Hutton M. Frequency of tau mutations in three series of non-Alzheimer's degenerative dementia. *Ann Neurol* 1999; **46**: 243–8
- Rizzu P, Van Swieten JC, Joosse M, Hasegawa M, Stevens M, Tibben A, Niermeijer MF, Hillebrand M, Ravid R, Oostra BA, Goedert M, van Duijn CM, Heutink P. High prevalence of mutations in the microtubule-associated protein tau in a population study of frontotemporal dementia in the Netherlands. *Am J Hum Genet* 1999; **64**: 414–21
- Rosso SM, Landweer EJ, Houterman M, Donker Kaat L, van Duijn CM, van Swieten JC. Medical and environmental risk factors for sporadic frontotemporal dementia: a retrospective case-control study. *J Neurol Neurosurg Psychiatry* 2003; **74**: 1574–6
- Mann DM. The neuropathology and molecular genetics of frontotemporal dementia. In *Dementia*, edition 2nd edn. Eds J O'Brien, D Ames, A Burns. London: Arnold, 2000: 759–68
- Reed LA, Wszolek ZK, Hutton M. Phenotypic correlations in FTDP-17. *Neurobiol Aging* 2001; **22**: 89–107
- Murrell JR, Spillantini MG, Zolo P, Guazzelli M, Smith MJ, Hasegawa M, Redi F, Crowther RA, Pietrini P, Ghetti B, Goedert M. Tau gene mutation G389R causes a tauopathy with abundant pick body-like inclusions and axonal deposits. *J Neuropathol Exp Neurol* 1999; **58**: 1207–26
- Ghetti B, Murrell JR, Zolo P, Spillantini MG, Goedert M. Progress in hereditary tauopathies: a mutation in the Tau gene (G389R) causes a Pick disease-like syndrome. *Ann N Y Acad Sci* 2000; **920**: 52–62
- Lippa CF, Zhukareva V, Kawarai T, Uryu K, Shafiq M, Nee LE, Grafman J, Liang Y, St George-Hyslop PH, Trojanowski JQ, Lee VM. Frontotemporal dementia with novel tau pathology and a Glu342Val tau mutation. *Ann Neurol* 2000; **48**: 850–8
- Pickering-Brown SM, Baker M, Yen S-H, Liu W-K, Hasegawa M, Cairns NJ, Lantos PL, Rossor M, Iwatsubo T, Davies Y, Allsop D, Furlong R, Owen F, Hardy J, Mann DMA, Hutton M. Pick's disease is associated with mutations in the tau gene. *Ann Neurol* 2000; **48**: 859–67
- Rizzini C, Goedert M, Hodges JR, Smith MJ, Jakes R, Hills R, Xuereb JH, Crowther RA, Spillantini MG. Tau gene mutation K257T causes a tauopathy similar to Pick's disease. *J Neuropathol Exp Neurol* 2000; **59**: 990–1001
- Neumann M, Schulz-Schaeffer W, Crowther RA, Smith MJ, Spillantini MG, Goedert M, Kretschmar HA. Pick's disease associated with the novel Tau gene mutation K369I. *Ann Neurol* 2001; **50**: 503–13
- Hayashi S, Toyoshima Y, Hasegawa M, Umeda Y, Wakabayashi K, Tokiguchi S, Iwatsubo T, Takahashi H. Late-onset frontotemporal dementia with a novel exon 1 (Arg5His) tau gene mutation. *Ann Neurol* 2002; **51**: 525–30
- Rosso SM, van Herpen E, Deelen W, Kamphorst W, Severijnen LA, Willemsen R, Ravid R, Niermeijer MF, Dooijes D, Smith MJ, Goedert M, Heutink P, van Swieten JC. A novel tau mutation, S320E, causes a tauopathy with inclusions similar to those in Pick's disease. *Ann Neurol* 2002; **51**: 373–6
- Hogg M, Gruijic ZM, Baker M, Demirci S, Guillozet AL, Sweet AP, Herzog LL, Weintraub S, Mesulam MM, LaPointe NE, Gambin TC, Berry RW, Binder LI, de Silva R, Lees A, Espinoza M, Davies P, Grover A, Sahara N, Ishizawa T, Dickson D, Yen SH, Hutton M, Bigio EH. The L266V tau mutation is associated with frontotemporal dementia and Pick-like 3R and 4R tauopathy. *Acta Neuropathol* 2003; **106**: 323–36

- 19 Pickering-Brown SM, Baker M, Nonaka T, Ikeda K, Sharma S, Mackenzie J, Simpson SA, Moore JW, Snowden JS, de Silva R, Revesz T, Hasegawa M, Hutton M, Mann DM. Frontotemporal dementia with Pick-type histology associated with Q336R mutation in the tau gene. *Brain* 2004; **127**: 1415–26
- 20 Wszolek Z, Pfeiffer RF, Bhatt MH, Schelper RL, Cordes M, Snow BJ, Rodnitsky RL, Wolters EC, Arwert F, Calne DB. Rapidly progressive autosomal dominant Parkinsonism and dementia with pallido-ponto-nigral degeneration. *Ann Neurol* 1992; **32**: 312–20
- 21 van Swieten JC, Stevens M, Rosso SM, Rizzo P, Joosse M, de Koning I, Kamphorst W, Ravid R, Spillantini MG, Niermeijer M, Heutink P. Phenotypic variation in hereditary frontotemporal dementia with tau mutations. *Ann Neurol* 1999; **46**: 617–26
- 22 Hasegawa M, Smith MJ, Iijima M, Tabira T, Goedert M. FTDP-17 mutations N279K and S305N in tau produce increased splicing of exon 10. *FEBS Lett* 1999; **443**: 93–6
- 23 Clark LN, Poorkaj P, Wszolek Z, Geschwind DH, Nasreddine ZS, Miller B, Li D, Payami H, Awert F, Markopoulou K, Andreadis A, D'Souza I, Lee VM, Reed L, Trojanowski JQ, Zhukareva V, Bird T, Schellenberg G, Wilhelmsen KC. Pathogenic implications of mutations in the tau gene in pallido-ponto-nigral degeneration and related neurodegenerative disorders linked to chromosome 17. *Proc Natl Acad Sci USA* 1998; **95**: 13103–7
- 24 Bugiani O, Murrell JR, Giaccone G, Hasegawa M, Ghigo G, Tabaton M, Morbin M, Primavera A, Carella F, Solaro C, Grisoli M, Savoiardo M, Spillantini MG, Tagliavini F, Goedert M, Ghetti B. Frontotemporal dementia and corticobasal degeneration in a family with a P301S mutation in tau. *J Neuropathol Exp Neurol* 1999; **58**: 667–77
- 25 Delisle MB, Murrell JR, Richardson R, Trofatter JA, Rascol O, Soulages X, Mohr M, Calvas P, Ghetti B. A mutation at codon 279 (N279K) in exon 10 of the Tau gene causes a tauopathy with dementia and supranuclear palsy. *Acta Neuropathol* 1999; **98**: 62–77
- 26 D'Souza I, Poorkaj P, Hong M, Nochlin D, Lee VM, Bird TD, Schellenberg GD. Missense and silent tau gene mutations cause frontotemporal dementia with parkinsonism-chromosome 17 type, by affecting multiple alternative RNA splicing regulatory elements. *Proc Natl Acad Sci USA* 1999; **96**: 5598–603
- 27 Goedert M, Spillantini MG, Crowther RA, Chen SG, Parchi P, Tabaton M, Lanska DJ, Markesbery WR, Wilhelmsen KC, Dickson DW, Petersen PB, Gambetti P. Tau gene mutation in familial progressive subcortical gliosis. *Nat Med* 1999; **5**: 454–7
- 28 Mirra SS, Murrell JR, Gearing M, Spillantini MG, Goedert M, Crowther RA, Levey AI, Jones R, Green J, Shoffner JM, Wainer BH, Schmidt ML, Trojanowski JQ, Ghetti B. Tau pathology in a family with dementia and a P301L mutation in tau. *J Neuropathol Exp Neurol* 1998; **58**: 335–45
- 29 Nasreddine ZS, Loginov M, Clark LN, Lamarche J, Miller BL, Lamontagne A, Zhukareva V, Lee VM, Wilhelmsen KC, Geschwind DH. From genotype to phenotype: a clinical pathological, and biochemical investigation of frontotemporal dementia and parkinsonism (FTDP-17) caused by the P301L tau mutation. *Ann Neurol* 1999; **45**: 704–15
- 30 Arima K, Kowalska A, Hasegawa M, Mukoyama M, Watanabe R, Kawai M, Takahashi K, Iwatsubo T, Tabira T, Sunohara N. Two brothers with frontotemporal dementia and parkinsonism with an N279K mutation of the tau gene. *Neurology* 2000; **54**: 1787–95
- 31 Spillantini MG, Yoshida H, Rizzini C, Lantos PL, Khan N, Rossor MN, Goedert M, Brown J. A novel tau mutation (N296N) in familial dementia with swollen achromatic neurons and corticobasal inclusion bodies. *Ann Neurol* 2000; **48**: 939–43
- 32 Stanford PM, Halliday GM, Brooks WS, Kwok JB, Storey CE, Creasey H, Morris JG, Fulham MJ, Schofield PR. Progressive supranuclear palsy pathology caused by a novel silent mutation in exon 10 of the tau gene: expansion of the disease phenotype caused by tau gene mutations. *Brain* 2000; **123**: 880–93
- 33 Iseki E, Matsumura T, Marui W, Hino H, Odawara T, Sugiyama N, Suzuki K, Sawada H, Arai T, Kosaka K. Familial frontotemporal dementia and parkinsonism with a novel N296H mutation in exon 10 of the tau gene and a widespread tau accumulation in the glial cells. *Acta Neuropathol* 2001; **102**: 285–92
- 34 Pickering-Brown SM, Richardson AM, Snowden JS, McDonagh AM, Burns A, Braude W, Baker M, Liu WK, Yen SH, Hardy J, Hutton M, Davies Y, Allsop D, Craufurd D, Neary D, Mann DM. Inherited frontotemporal dementia in nine British families associated with intronic mutations in the tau gene. *Brain* 2002; **125**: 732–51
- 35 Grover A, DeTure M, Yen SH, Hutton M. Effects on splicing and protein function of three mutations in codon N296 of tau in vitro. *Neurosci Lett* 2002; **323**: 33–6
- 36 Halliday GM, Song YJC, Creasey H, Morris JG, Brooks WS, Kriji J. Neuropathology in the S305S tau gene mutation. *Brain* 2006 (in press)
- 37 Taniguchi S, McDonagh AM, Pickering-Brown SM, Umeda Y, Iwatsubo T, Hasegawa M, Mann DM. The neuropathology of frontotemporal lobar degeneration with respect to the cytological and biochemical characteristics of tau protein. *Neuropathol Appl Neurobiol* 2004; **30**: 1–18
- 38 Mirra SS, Heyman A, McKeel D, Sumi SM, Crain BJ, Brownlee LM, Vogel FS, Hughes JP, van Belle G, Berg L. The Consortium to Establish a Registry for Alzheimer's Disease (CERAD). Part II. Standardization of the neuropathologic assessment of Alzheimer's disease. *Neurology* 1991; **41**: 479–86
- 39 Braak H, Braak E. Neuropathological staging of Alzheimer-related changes. *Acta Neuropathol* 1991; **82**: 239–59
- 40 Kertesz A, McGonagle P, Blair M, Davidson W, Munoz DG. The evolution and pathology of frontotemporal dementia. *Brain* 2005; **128**: 1996–2005

- 41 McKhann GM, Albert MS, Grossman M, Miller B, Dickson D, Trojanowski JQ. Workgroup on Frontotemporal dementia and Pick's disease. Clinical and pathological diagnosis of frontotemporal dementia: report of the workgroup on Frontotemporal dementia and Pick's disease. *Arch Neurol* 2001; **59**: 1203-4
- 42 Goedert M, Jakes R, Crowther RA, Six J, Lubke U, Vandermeeren M, Cras P, Trojanowski JQ, Lee VM. The abnormal phosphorylation of tau protein at Ser-202 in Alzheimer disease recapitulates phosphorylation during development. *Proc Natl Acad Sci USA* 1993; **90**: 5066-70
- 43 Mercken M, Vandermeeren M, Lubke U, Six J, Boons J, Van de Voorde A, Martin JJ, Gheuens J. Monoclonal antibodies with selective specificity for Alzheimer Tau are directed against phosphatase-sensitive epitopes. *Acta Neuropathol* 1992; **84**: 265-72
- 44 Goedert M, Jakes R, Crowther RA, Cohen P, Vanmechelen E, Vandermeeren M, Cras P. Epitope mapping of monoclonal antibodies to the paired helical filaments of Alzheimer's disease: identification of phosphorylation sites in tau protein. *Biochem J* 1994; **301**: 871-7
- 45 Mann DM, McDonagh AM, Pickering-Brown SM, Kowa H, Iwatsubo T. Amyloid beta protein deposition in patients with frontotemporal lobar degeneration: relationship to age and apolipoprotein E genotype. *Neurosci Lett* 2001; **304**: 161-4
- 46 Kondo J, Honda T, Mori H, Hamada Y, Miura R, Ogawara M, Ihara Y. The carboxyl third of tau is tightly bound to paired helical filaments. *Neuron* 1988; **1**: 827-34
- 47 Kosik KS, Orecchio LD, Binder L, Trojanowski JQ, Lee VM, Lee G. Epitopes that span the tau molecule are shared with paired helical filaments. *Neuron* 1988; **1**: 817-25
- 48 Zheng-Fischhofer Q, Biernat J, Mandelkow EM, Illenberger S, Godemann R, Mandelkow E. Sequential phosphorylation of Tau by glycogen synthase kinase-3 β and protein kinase A at Thr212 and Ser214 generates the Alzheimer-specific epitope of antibody AT100 and requires a paired-helical-filament-like conformation. *Eur J Biochem* 1998; **252**: 542-52
- 49 Mailliot C, Sergeant N, Bussièrre N, Caillet-Boudin ML, Delacourte A, Buee L. Phosphorylation of specific sets of tau isoforms reflects different neurofibrillary degeneration processes. *FEBS Lett* 1998; **433**: 201-4
- 50 Probst A, Tolnay M, Langui D, Goedert M, Spillantini MG. Pick's disease: hyperphosphorylated tau protein segregates to the somatoaxonal compartment. *Acta Neuropathol* 1996; **92**: 588-96
- 51 Augustinack JC, Schneider A, Mandelkow EM, Hyman BT. Specific tau phosphorylation sites correlate with severity of neuronal cytopathology in Alzheimer's Disease. *Acta Neuropathol* 2002; **103**: 26-35
- 52 Ferrer L, Barrachina M, Puig B. Anti-tau phosphospecific Ser²⁰² antibody recognises a variety of abnormal hyperphosphorylated tau deposits in tauopathies including Pick bodies and argyrophilic grains. *Acta Neuropathol* 2002; **104**: 658-64
- 53 Goedert M, Spillantini MG, Cairns NJ, Crowther RA. Tau proteins of Alzheimer paired helical filaments: abnormal phosphorylation of all six brain isoforms. *Neuron* 1992; **8**: 159-68
- 54 Alonso AC, Grundke-Iqbal I, Iqbal K. Alzheimer's disease hyperphosphorylated tau sequesters normal tau into tangles of filaments and disassembles microtubules. *Nat Med* 1996; **2**: 783-7
- 55 Alonso AC, Mederlyova A, Novak M, Grundke-Iqbal I, Iqbal K. Promotion of hyperphosphorylation by frontotemporal dementia tau mutations. *J Biol Chem* 2004; **279**: 34873-81
- 56 Iqbal K, Alonso Adel C, Chen S, Chohan MO, El-Akkad E, Gong CX, Khatoun S, Li B, Liu F, Rahman A, Tanimukai H, Grundke-Iqbal I. Tau pathology in Alzheimer disease and other tauopathies. *Biochim Biophys Acta* 2005; **1739**: 198-210
- 57 Sumpter PQ, Mann DMA, Davies CA, Yates PO, Snowden JS, Neary D. An ultrastructural analysis of the effects of accumulation of neurofibrillary tangle in pyramidal cells of the cerebral cortex in Alzheimer's disease. *Neuropathol Appl Neurobiol* 1986; **12**: 305-19
- 58 Smith MA, Siedlak SL, Richey PL, Nagaraj RH, Elhammer A, Perry G. Quantitative solubilization and analysis of insoluble paired helical filaments from Alzheimer disease. *Brain Res* 1996; **717**: 99-108
- 59 Jicha GA, Lane E, Vincent I, Otvos L Jr, Hoffmann R, Davies P. A conformation- and phosphorylation-dependent antibody recognizing the paired helical filaments of Alzheimer's disease. *J Neurochem* 1997; **69**: 2087-95
- 60 Wechsler AF, Verity MA, Rosenschein S, Fried I, Scheibel AB. Pick's disease. A clinical, computed tomographic, and histologic study with golgi impregnation observations. *Arch Neurol* 1982; **39**: 287-90

Received 12 September 2005

Accepted after revision 24 January 2006

Rohan de Silva · Tammaryn Lashley
Catherine Strand · Anna-Maria Shiarli
Jing Shi · Jinzhou Tian · Kathryn L. Bailey
Peter Davies · Eileen H. Bigio · Kunimasa Arima
Eizo Iseki · Shigeo Murayama · Hans Kretschmar
Manuela Neumann · Carol Lippa · Glenda Halliday
James MacKenzie · Rivka Ravid · Dennis Dickson
Zbigniew Wszolek · Takeshi Iwatsubo
Stuart M. Pickering-Brown · Janice Holton
Andrew Lees · Tamas Revesz · David M. A. Mann

An immunohistochemical study of cases of sporadic and inherited frontotemporal lobar degeneration using 3R- and 4R-specific tau monoclonal antibodies

Received: 2 December 2005 / Revised: 20 January 2006 / Accepted: 21 January 2006 / Published online: 22 March 2006
© Springer-Verlag 2006

Abstract The pathological distinctions between the various clinical and pathological manifestations of frontotemporal lobar degeneration (FTLD) remain

unclear. Using monoclonal antibodies specific for 3- and 4-repeat isoforms of the microtubule associated protein, tau (3R- and 4R-tau), we have performed an

R. de Silva · A. Lees
Reta Lila Weston Institute of Neurological Studies,
University College London, Windeyer Building,
46 Cleveland St, W1T 4JF, London, UK

T. Lashley · C. Strand · J. Holton · T. Revesz
Department of Molecular Neuroscience,
Queen Square Brain Bank, Institute of Neurology,
University College London, Queen Square,
WC1N 3BG, London, UK

A.-M. Shiarli · J. Shi · J. Tian · K. L. Bailey
S. M. Pickering-Brown · D. M. A. Mann (✉)
Centre for Clinical Neurosciences, University of Manchester,
Greater Manchester Neurosciences Centre, Hope Hospital,
M6 8HD, Salford, UK
E-mail: david.mann@manchester.ac.uk
Tel.: +44-161-2062580
Fax: +44-161-2060388

J. Shi · J. Tian
Department of Care of the Elderly,
Dongzhimen Hospital,
100700, Beijing, P R China

P. Davies
Department of Pathology, Albert Einstein College of Medicine,
Bronx, NY, 10461, USA

E. H. Bigio
Northwestern University Alzheimer's Disease Center,
Chicago, IL, 60611, USA

K. Arima
National Centre of Neurology and Psychiatry,
Musashi Hospital, 187-8551, Tokyo, Japan

E. Iseki
Juntendo Tokyo Koto Geriatric Medical Center,
Juntendo University School of Medicine, 136-0075, Tokyo, Japan

S. Murayama
Department of Neuropathology, Tokyo Metropolitan
Institute of Gerontology, 173, Tokyo, Japan

H. Kretschmar · M. Neumann
Reference Centre for Prion Diseases and Neurodegenerative
Diseases, Institute of Neuropathology, Marchioninstr. 17,
81377, Munchen, Germany

C. Lippa
Memory Disorders Centre, Drexel University College of Medicine,
Philadelphia, PA, 19129, USA

G. Halliday
Department of Neuropathology,
Prince of Wales Medical Research Institute,
University of New South Wales, NSW 2031, Randwick, Australia

J. MacKenzie
The Royal Infirmary, Foresterhill, AB25 2ZD, Aberdeen, Scotland

R. Ravid
Netherlands Brain Bank, Meibergdreef 33,
1105 AZ, The Netherlands

D. Dickson · Z. Wszolek · S. M. Pickering-Brown
Mayo Clinic, 4500 San Pablo Rd,
Jacksonville, FL, 32224, USA

T. Iwatsubo
Department of Neuropathology and Neuroscience,
University of Tokyo, 113-0033, Tokyo, Japan

immunohistochemical study of the tau pathology present in 14 cases of sporadic forms of FTLT, 12 cases with Pick bodies and two cases without and in 27 cases of familial FTLT associated with 12 different mutations in the tau gene (*MAPT*), five cases with Pick bodies and 22 cases without. In all 12 cases of sporadic FTLT where Pick bodies were present, these contained only 3R-tau isoforms. Clinically, ten of these cases had frontotemporal dementia and two had progressive apraxia. Only 3R-tau isoforms were present in Pick bodies in those patients with familial FTLT associated with L266V, Q336R, E342V, K369I or G389R *MAPT* mutations. Patients with familial FTLT associated with exon 10 N279K, N296H or +16 splice site mutations showed tau pathology characterised by neuronal neurofibrillary tangles (NFT) and glial cell tangles that contained only 4R-tau isoforms, as did the NFT in P301L *MAPT* mutation. With the R406W mutation, NFT contained both 3R- and 4R-tau isoforms. We also observed two patients with sporadic FTLT, but without Pick bodies, in whom the tau pathology comprised only of 4R-tau isoforms. We have therefore shown by immunohistochemistry that different specific tau isoform compositions underlie the various kinds of tau pathology present in sporadic and familial FTLT. The use of such tau isoform specific antibodies may refine pathological criteria underpinning FTLT.

Introduction

Frontotemporal lobar degeneration (FTLD) describes a clinically and pathologically heterogeneous group of forms of dementia that have onset of illness usually between ages of 35 and 75 years and affect males and females equally [41, 56]. A previous family history of a similar disorder occurs in about half of patients [41, 53, 56] and in many such familial cases a mutation in the gene encoding the microtubule associated protein, tau (*MAPT*) on chromosome 17 seems causal (see Ref. [15, 32] for recent reviews). To date, about 35 causal *MAPT* mutations in around 150 families have been identified and the term frontotemporal dementia with parkinsonism linked to chromosome 17 (FTDP-17) was adopted [12] to accommodate the clinical and genetic features of such cases. At autopsy, patients with FTLT generally show atrophy of the frontal and temporal lobes of the brain associated with a degeneration and loss of large pyramidal neurons from such regions irrespective of clinical subtype or family history [41, 56]. However, under this umbrella of pathological change, histopathological differences occur [41, 55, 62] and over the years there have been several attempts at classification based upon microscopic appearances.

In the first case reports, made over a century ago by Arnold Pick, the characterising features of intraneuronal argyrophilic inclusions (Pick bodies) and swollen or ballooned neurons (Pick cells) were described and the eponym Pick's disease was coined to distinguish

such cases from those of Alzheimer's disease where senile plaques and neurofibrillary tangles were the key pathology. However, recognizing that clinically similar forms of FTLT occurred without such Pick- or Alzheimer-type changes being present led to the scheme by Constantinidis [7] in which three variants of FTLT were identified: one with Pick bodies and Pick cells (type A), one with only Pick cells (type B) and one with neither (type C). Later immunohistochemical studies [33] indicated either a Pick-type of histology based on the presence of tau-positive Pick bodies (equivalent to Constantinidis type A) or a microvacuolar-type histology in which no tau intraneuronal inclusions (Pick bodies) were seen (equivalent to Constantinidis types B and C). Recent surveys [22, 31, 37, 41, 55, 62] indicate that about half of cases of FTLT show a histopathology based on the accumulation of insoluble aggregates of tau protein within neurons and glial cells of the cerebral cortex and hippocampus. In most other cases, termed FTLT-U, tau negative but ubiquitin positive inclusions usually occur within cerebral cortex and hippocampus and when clinical motor neuron disease (MND) is also present the term FTLT-MND can be ascribed. Sometimes, neither tau nor ubiquitin inclusions are seen; such cases have been labelled as dementia lacking distinctive histology. These observations are broadly in line with the recommendations of a consensus conference held in 2001 in an attempt to establish internationally accepted clinical and neuropathological criteria for FTLT [34]. Nonetheless, at the time such criteria were put forward it was recognized that they were likely to be interim and subject to review in the light of expanding knowledge of this disorder—a point reiterated in some most recent surveys [37, 55].

Tau-based pathology in FTLT can occur in either sporadic or familial cases. In sporadic cases of FTLT, tau pathology usually takes the form of Pick bodies and Pick cells, though in such cases some tau positive glial cells and dystrophic neurites can often be seen [66], though if cases of corticobasal degeneration (CBD), progressive supranuclear palsy (PSP) or argyrophilic grain disease are included under the rubric of FTLT as has been the case in certain recent surveys [22, 31, 37] a neurofibrillary tangle-based tau pathology becomes more common.

In some familial cases (i.e., those with FTDP-17) with missense mutations within coding regions of exons 1, 9, 11, 12 and 13 of *MAPT* there are swollen nerve cells and rounded neuronal inclusions within large and small pyramidal neurones of the cerebral cortex and pyramidal and granule cells of the hippocampus reminiscent of the Pick bodies seen in sporadic disease [4, 14, 23, 29, 30, 39, 42, 45, 47, 50, 52]. Such mutations affect all six isoforms of tau, generating mutated tau molecules that (variably) lose their ability to interact with microtubules [20, 21, 23, 39, 42, 50, 51], increasing their propensity to self-aggregate into fibrils [20, 21, 23, 42, 47, 51]. Other *MAPT* mutations cluster around, or

lie within a predicted regulatory stem loop structure of a splice acceptor domain of *MAPT* pre-mRNA that determines the inclusion or exclusion of exon 10 by alternative splicing during gene transcription [2, 3, 5, 6, 9, 11, 17, 19, 20, 24, 25, 35, 40, 43, 46, 48, 52, 58–60], destabilizing the stem loop [24, 58] or strengthening [11, 18, 20] or destroying [11] splice enhancing, or splice silencing [11, 59] elements in the 5' region of exon 10. Such cases show insoluble aggregated tau deposits as neurofibrillary tangle-like structures within large and smaller pyramidal cells of cortical layers III and V and prominently within glial cells in the deep white matter, globus pallidus and internal capsule [2, 17, 19, 35, 43, 46, 51, 58–60]. However, other exon 10 mutations do not affect the splicing of exon 10 [11, 24] but induce conformational changes in tau molecules containing exon 10 that interfere with microtubule function and lead to aggregation of the mutated tau into neurofibrillary tangles [18, 36, 59].

Although the brain tau isoform composition has been extensively analysed by western blotting both in cases of sporadic FTLD where Pick bodies [1, 8, 37, 53, 61, 65] or Pick-like bodies [37] are present and in many of the cases with FTDP-17 [2–6, 9, 14, 17, 19, 23, 25, 29, 30, 35, 36, 39, 42, 43, 45–47, 50, 52, 59, 60, 62, 65], certain ambiguities remain. For example, in cases of sporadic FTLD where Pick bodies are seen in histology, most western blotting studies have detected only tau isoforms with 3-repeat microtubule binding domains (3R-tau) [8, 37, 54], though other investigations have shown certain cases to show tau isoforms with both 3R-tau and 4-repeat microtubule binding domains (4R-tau) [1, 37, 62, 66] and in yet others only 4R-tau is seen [37, 62, 66]. Such disparities have led to controversies as to whether Pick bodies are composed of only 3R-tau, only 4R-tau or an admixture of 3R- and 4R-tau isoforms. Similarly, in some cases of FTDP-17 with Pick bodies (e.g., K257T *MAPT* mutation Ref. [50]) western blotting has likewise shown only 3R-tau to be present, whereas in other cases (e.g., L266V, G272V, G342V and G389R *MAPT* mutations) both 3R-tau and 4R-tau isoforms are seen [4, 14, 23, 31, 45]. One possible explanation for these apparent inconsistencies may lie in differing anatomical compartmentalizations of 3R- and 4R-tau isoforms between cases, a distinction that is lost upon the tissue homogenization required for western blotting. Specific immunohistological patterns associated with 3R- and 4R-tau isoforms cannot be distinguished using phospho-dependent and phospho-independent tau antibodies that recognize tau epitopes shared by all six tau isoforms.

In the present study, therefore, we have investigated in situ, using monoclonal antibodies specific for 3R- and 4R-tau isoform species, the isoform composition of the tau histopathological changes in 14 cases of sporadic FTLD and 27 cases of familial FTLD associated with 11 different mutations in *MAPT*, for which tau isoform patterns on western blotting have already

been reported, in order to reconcile such inconsistencies and to provide further insight into disease classification by the use of tau antibodies not available when the last pathological criteria [34] were proposed.

Materials and methods

Brain tissues from 14 cases with sporadic FTLD (cases #1–14), in 12 of whom (cases #1–12) previous pathological investigations had shown Pick bodies to be present and five cases of familial FTLD (cases #30–34) with exon 10 + 16 *MAPT* mutation were obtained from the Manchester Brain Bank. Seven of the sporadic FTLD cases (cases #1, 2, 4–7 and 13) had been included (as cases # 4–8, 10 and 12, respectively) in a previous study [66] investigating tau isoform composition in a series of 14 cases of FTLD. Eight of the sporadic FTLD cases (cases #1, 2, 4–7, 9 and 13) had been included (as cases #10, 11, 12, 13, 14, 15, 17 and 16, respectively) in a previous study of ours [62] also investigating tau isoform composition in FTLD. Tissues from the other 22 familial FTLD cases with *MAPT* mutations were kindly supplied in collaboration by colleagues from different centres across the world. Selected clinical and pathological details for all cases are given in Table 1. Full clinical and pathological descriptions for 25 of the 27 cases with *MAPT* mutations have been previously reported by the originating authors (see Table 1 for details of citation); the other two cases remain unreported to date.

Serial sections were cut at a thickness of 6 μ m from formalin-fixed, wax-embedded blocks of frontal cortex (BA 8/9) from all 14 sporadic FTLD cases and 27 familial FTLD cases with *MAPT* mutations and from temporal cortex (BA 21/22) to include the hippocampus in the 14 sporadic FTLD cases alone and mounted onto APES-coated slides. One set of sections was immunostained for insoluble pathological tau proteins by a standard immunoperoxidase method using the phospho-dependent tau antibody AT8 (1:750) (Innogenetics, Belgium). AT8 antibody is raised against the phosphorylated Ser 202/Thr 205 epitope and immunoreacts with PHF-tau in AD [16]. It will detect all isoforms of tau in which this epitope is phosphorylated. Other sets of sections were stained with the 3R-tau specific monoclonal antibody RD3 [10] (1:3000; Upstate, Dundee, UK) and the 4R-tau specific monoclonal antibody ET3 (gift of P Davies, 1:100) as described [10]. Briefly, sections were deparaffinised in xylene and rehydrated in decreasing concentrations of alcohol. Endogenous peroxidase activity was blocked with 0.3% H₂O₂ in methanol for 10 min. Sections were pressure cooked for 10 min in 0.01 M citrate buffer pH6.0. Sections were incubated in 10% non-fat milk to block non-specific staining, then with the primary antibodies RD3 and ET3 for 1 h at room temperature. This was followed by several washes in PBS and treatment with biotinylated

Table 1 Selected clinical and pathological details

Case	Pathology	MAPT mutation	Gender	Onset (years)	Death (years)	Duration (years)	APOE genotype	Brain weight (g)
1 [55, 62]	Pick bodies	None	F	53	60	7	3.3	960
2 [55, 62]	Pick bodies	None	M	46	56	10	3.3	1,150
3 [55, 62]	Pick bodies	None	M	54	63	9	n.a.	n.a.
4 [55, 62]	Pick bodies	None	F	52	62	10	3.4	928
5 [55, 62]	Pick bodies	None	F	76	84	8	3.3	1,235
6 [55, 62]	Pick bodies	None	F	50	58	8	2.2	1,065
7 [55, 62]	Pick bodies	None	M	63	74	11	2.3	990
8 [55, 62]	Pick bodies	None	M	73	77	4	3.3	n.a.
9 [55, 62]	Pick bodies	None	M	47	61	14	3.4	980
10 [55, 62]	Pick bodies	None	M	59	69	10	3.3	885
11 [55, 62]	Pick bodies	None	M	55	67	12	3.3	895
12 [55, 62]	Pick bodies	None	F	51	57	6	3.3	1,210
13 [55, 62]	NFT-like	None	F	57	64	7	3.3	1,000
14 [55, 62]	NFT-like	None	F	64	70	6	3.3	1,090
15 [23]	Pick bodies	L266V	M	32	36	3.5	n.a.	1,050
16 [2]	NFT, glial tangles	N279K	M	46	57	11	3.3	1,250
17 [2]	NFT, glial tangles	N279K	M	44	50	6	3.3	1,420
18 [6, 64]	NFT, glial tangles	N279K	M	44	50	6	3.4	1,290
19 [6, 64]	NFT, glial tangles	N279K	F	45	48	3	3.3	1,100
20 [6, 64]	NFT, glial tangles	N279K	M	56	58	2	2.3	1,400
21 [6, 64]	NFT, glial tangles	N279K	F	45	53	8	2.4	1,000
22 [6, 64]	NFT, glial tangles	N279K	M	57	63	6	3.4	1,100
23 [6, 64]	NFT, glial tangles	N279K	M	41	52	11	2.3	1,100
24 [25]	NFT, glial tangles	N296H	F	57	62	3	3.3	960
25 [51, 63]	NFT	P301L	M	~48	60	>12	3.3	1,331
26 [51, 63]	NFT	P301L	M	44	52	8	2.3	1,087
27 [51, 63]	NFT	P301L	F	54	76	22	2.2	1,006
28 [51, 63]	NFT	P301L	F	59	64	5	3.3	1,013
29 [19, 60]	NFT, glial tangles	S305S	F	48	51	3	n.a.	1,053
30 [46]	NFT, glial tangles	Exon 10 +16	M	50	61	11	3.4	1,016
31 [46]	NFT, glial tangles	Exon 10 +16	F	46	58	12	3.3	996
32 [46]	NFT, glial tangles	Exon 10 +16	M	43	55	12	3.4	1,240
33 [46]	NFT, glial tangles	Exon 10 +16	F	52	65	13	2.3	1,040
34 [46]	NFT, glial tangles	Exon 10 +16	F	48	56	8	3.4	1,175
35 ^{uc}	NFT, glial tangles	Exon 10 +16	M	57	63	6	3.3	1,440
36 [47]	Pick bodies	Q336R	M	58	68	10	3.3	1,102
37 [30]	Pick bodies	E342V	F	48	55	7	3.3	1,020
38 [42]	Pick bodies	K369I	F	52	61	9	n.a.	885
39 ^{uc}	Pick bodies	G389R	M	45	49	4	n.a.	1,170
40 [51, 63]	NFT	R406W	M	63	70	7	3.3	1,121
41 [51, 63]	NFT	R406W	F	58	71	13	3.4	905

Superscript indicates case reference

^{uc}Indicates unpublished case

NFT neurofibrillary tangle, *n.a.* APOE genotype or brain weight not available

anti-mouse (Dako 1:200) for 30 min and ABC (Dako) for 30 min. Peroxidase activity was developed with diaminobenzidine/ H₂O₂ solution [10].

The specificity of ET3 has been demonstrated previously in Western blots of recombinant 3R- and 4R-tau [27]. It has also been characterised in immunohistochemical studies of argyrophilic grain disease [13] and other tauopathies [23].

Results

Sporadic FTLD

Semi-quantitative rating data for AT8, ET3 and RD3 immunostaining in the 14 sporadic FTLD cases is given in Table 2.

Cases with Pick bodies

Of the 14 cases with sporadic FTLD, 12 cases (cases #1–12) displayed Pick-type histology. Pick bodies were identified as defined by Kertesz et al. [28], as round or oval, compact intracytoplasmic neuronal inclusions, stained by Bielschowsky but not by Gallyas, tau-immunoreactive and located in dentate fascia, hippocampus and cerebral cortex. Clinically, nine cases (cases #1–7, 9 and 10) showed typical frontotemporal dementia, whereas case #8 had suffered from progressive aphasia and cases #11 and 12 from progressive apraxia. In 11 of these 12 cases (cases #1–4, 6–12), numerous Pick bodies were widespread within frontal and temporal cortex, chiefly in layers two and four and within dentate gyrus granule cells (Fig. 1a) and pyramidal cells of the

Table 2 Frequency of tau-immunoreactive pathological changes in frontal and temporal cortex and hippocampus, as detected in 14 patients with sporadic FTLD using AT8 (all tau isoforms), ET3 (4R-tau isoforms only) and RD3 (3R-tau isoforms only) antibodies

Case	Frontal			Temporal			Hippocampus			Tau biochemistry
	AT8	ET3	RD3	AT8	ET3	RD3	AT8	ET3	RD3	
1a	++++	0	+++	++++	0	++++	++++	0	++++	n.d.
2a	++++	0	+++	+++	0	+++	+++	0	+++	Mostly 3R, trace 4R [62, 66]
3 ^a	++++	0	+++	++++	0	++++	++++	0	+++	n.d.
4 ^a	++++	0	+++	++++	0	++++	+++	0	+++	Mostly 3R, trace 4R [62, 66]
5 ^{a,b}	+	0	0/+	+++	0	0/+	++++	0	+++	Mainly 4R, some 3R [62, 66]
6 ^a	++++	0	+++	++++	0	++++	++++	0	+++	Mostly 3R, trace 4R [62, 66]
7 ^a	+++	0	++	+++	0	+	++++	0	+++	n.d.
8 ^a	++++	0	+++	++	0	+	++++	0	+++	n.d.
9 ^a	++++	0	+++	++++	0	++++	++++	0	+++	Mostly 3R, trace 4R [62, 66]
10 ^a	++++	0	+++	++++	0	++++	++++	0	+++	n.d.
11 ^a	++	0	+	+++	0	+++	++++	0	+++	n.d.
12 ^a	+++	0	++	++++	0	+++	++++	0	+++	n.d.
13 ^b	+++	++	0	+++	+	0	+	0/+	0	Mainly 4R [62, 66]
14 ^b	+	0/+	0	++	+	0/+	+++	+	0	n.d.

Tau biochemical findings are shown (where known)

0 absent, 0/+ rare, + few, ++ moderate number, +++ many, ++++ very many

^aPick bodies

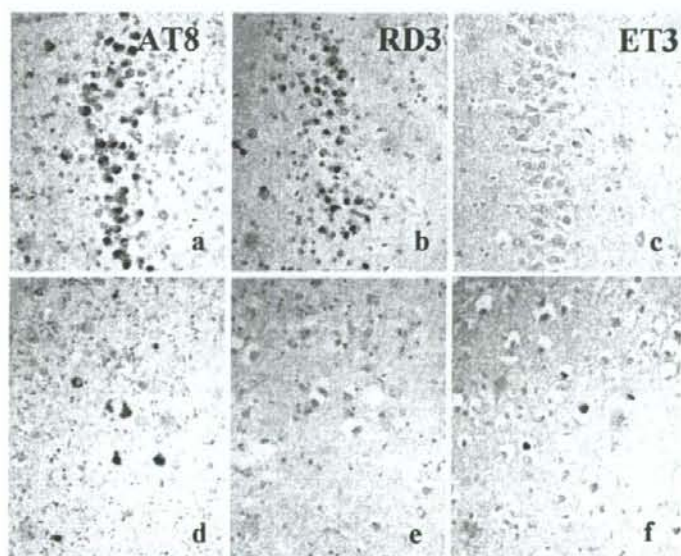
^bNeurofibrillary tangle-like structures, 3R 3-repeat tau, 4R 4-repeat tau, n.d. not done

hippocampus. However, in one elderly case (aged 83 years) (case #5) Pick bodies were widely present only in the granule cells of the dentate gyrus and pyramidal cells of the hippocampus, but less so within temporal neocortex. In this case occasional neurons showing diffuse cytoplasmic tau immunoreactivity (pretangles) and neurofibrillary tangle-like structures were seen in the frontal and temporal cortex (see also two cases reported by Mott et al. [37]). No other cases displayed such AD-type neurofibrillary changes. In cases #3, 4, 6 and 9,

AT8-immunoreactive astrocytes were present within the cerebral cortex and white matter and a fine meshwork of dystrophic neurites (threads) was seen. These findings are typical of those seen using anti-tau antibodies such as AT8 which detect all hyperphosphorylated isoforms of tau and have been described on many occasions previously (e.g., Ref. [62, 66]).

In all 12 cases, the Pick bodies were strongly stained with RD3 antibody (Fig. 1b), usually to approximately the same extent as with AT8, but none were stained with

Fig. 1 Tau pathology in patients with sporadic FTLD. In patient #4 (a-c) Pick bodies within granule cells of the dentate gyrus of the hippocampus are immunoreactive with AT8 (a) and RD3 (b) antibodies, but not with ET3 (c) antibody. In patient #13 without Pick bodies (d-f) neurons with amorphous tau deposits or neurofibrillary tangle-like structures are immunoreactive with AT8 (d) and ET3 (f) antibodies, but not with RD3 antibody (e). Immunoperoxidase-haematoxylin, AT8 antibody (a, d), RD3 antibody (b, e), ET3 antibody (c, f). All 250 times microscope magnification



ET3 (Fig. 1c). In case #5 a minority of the Pick bodies within temporal neocortex were also stained with RD3, as were a few of the NFT-like structures in the frontal cortex, though neither were stained with ET3. In case #6 rare glial cells were diffusely stained with ET3.

Cases without Pick bodies

In the other two sporadic FTLD cases (cases #13 and 14) typical Pick bodies were absent from hippocampal dentate gyrus granule cells and pyramidal cells. In these, AT8 staining revealed numerous cells in both hippocampal regions containing fine, granular deposits of tau protein, which sometimes had NFT-like appearance. In both cases a few of the pyramidal cells, but none of the dentate gyrus granule cells, were stained with ET3, but not RD3, antibody. In frontal and temporal cortex fine amorphous deposits of tau protein which sometimes adopted a rounded, ring or crescent shape, other times a more NFT-like structure, were seen with AT8 staining (Fig. 1d). The amorphous tau deposits were sometimes similarly stained with RD3 and may be associated with ribosomes (Nissl bodies) (see also Papasozomenos Ref. [44]), whereas the rounded, ring or crescent shaped

inclusions were only stained with ET3 (Fig. 1f) and not RD3 (Fig. 1e). In neither case were glial cell inclusions, or astrocytic plaques, of the type seen in CBD, present. These cases presented clinically with FTD and showed no features to distinguish them from the other 12 sporadic FTLD cases.

Familial FTLD

Semi-quantitative rating data for AT8, ET3 and RD3 immunostaining in the 27 familial FTLD cases is given in Table 3.

MAPT mutations in exons 9, 12 and 13

In cases #15 (exon 9, L266V), #36 (exon 12, Q336R), #37 (exon 12, E342V) and #38 (exon 12, K369I), many neurons containing diffuse deposits of tau protein were seen in frontal cortex in AT8 immunostained sections. In some cells, in each mutation, the insoluble tau was aggregated into rounded structures resembling the Pick bodies seen in the sporadic FTLD cases (Fig. 2a). These Pick-like bodies were likewise stained with RD3 anti-

Table 3 Frequency of tau-immunoreactive pathological changes in frontal cortex as detected in 27 patients with familial FTLD with *MAPT* mutations using AT8 (all tau isoforms), ET3 (4R-tau isoforms only) and RD3 (3R-tau isoforms only) antibodies

Case	<i>MAPT</i> mutation	AT8	ET3	RD3	Tau biochemistry
15 ^{a,d}	L266V	++++ ^{a,d}	+ ^d	++++ ^a	Mostly 3R[2]
16 ^c	N279K	+++	+	0	4R only [2]
17 ^c	N279K	+++	+++	0	4R only [2]
18 ^c	N279K	+++	++	0	4R only [6]
19 ^c	N279K	+++	+	0	4R only [6]
20 ^f	N279K	+++	++	0	4R only [6]
21 ^c	N279K	+++	++	0	4R only [6]
22 ^c	N279K	++++	+++	0	4R only [6]
23 ^c	N279K	++++	+++	0	4R only [6]
24 ^c	N296H	++++	+++	0	4R only [25]
25 ^b	P301L	++++	+	0	4R only [51, 63]
26 ^{b,e}	P301L	+++	++	0	4R only [51, 63]
27 ^{b,e}	P301L	++++	0	0/+	4R only [51, 63]
28 ^{b,e}	P301L	++++	+++	+	4R only [51, 63]
29 ^c	S305S	++	+++	0	4R only [19]
30 ^c	Exon 10+16	+	0/+	0	n.d.
31 ^c	Exon 10+16	+++	+	0	4R only [46]
32 ^c	Exon 10+16	+++	++	0	4R only [46]
33 ^c	Exon 10+16	++++	++++	0	n.d.
34 ^c	Exon 10+16	++++	+++	0/+	n.d.
35 ^c	Exon 10+16	+++	++	0	n.d.
36 ^a	Q336R	++++	0/+	+++	n.d.
37 ^{a,d}	E342V	++++ ^{a,d}	0/+ ^d	+ ^a	Mostly 4R [30]
38 ^a	K369I	++++	0	+++	3R and 4R [42]
39 ^a	G389R	++	0	+	n.d.
40 ^b	R406W	+++	+++	+++	3R and 4R [51, 63]
41 ^b	R406W	+++	++	++	3R and 4R [51, 63]

Tau biochemical findings are shown (where known)

^aPick bodies present in neurones

^bNeurofibrillary tangle-like structures in neurones

^cNeurofibrillary tangle-like structures in neurons with glial cell tangles in white matter

^dGlia in grey matter staining

^eSome diffuse β -amyloid plaques, - absent, 0/+ rare, + few, ++ moderate number, +++ many, ++++ very many, 3R 3-repeat tau, 4R 4-repeat tau, n.d. not done

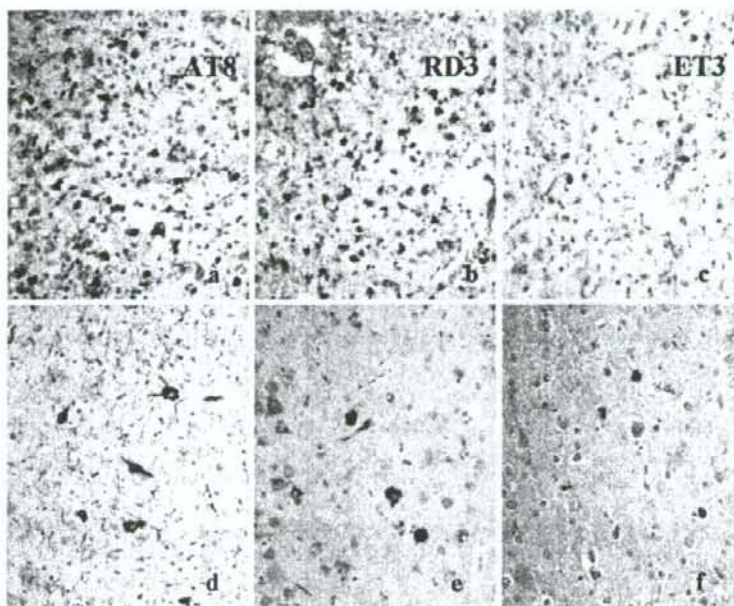


Fig. 2 Tau pathology in patients with familial FTL. In patient #15 with *MAPT* L266V mutation (a-c), Pick bodies within pyramidal cells of the frontal cortex are immunoreactive with AT8 (a) and RD3 (b) antibodies, but not with ET3 (c) antibody. However, there are also numerous astrocytes within grey matter of frontal cortex that are immunoreactive with AT8 antibody (a), some of which are also reactive with ET3 antibody (c), but not with RD3 (b) antibody. In patient #40 with *MAPT* R406W mutation

(d-f) neurones show amorphous tau deposits or neurofibrillary tangle-like structures that are immunoreactive with AT8 (d), RD3 (e) and ET3 (f) antibodies. In this patient numerous neuropil threads are seen but these are reactive only with AT8 antibody (d). Immunoperoxidase-haematoxylin, AT8 antibody (a, d), RD3 antibody (b, e), ET3 antibody (c, f). All 250 times microscope magnification

body (Fig. 2b) but not (or only very rarely so) with ET3 antibody (Fig. 2c). However, in L266V and E342V *MAPT* mutations numerous diffusely stained astrocytes were seen with AT8 antibody (Fig. 2a). These were also stained with ET3 (Fig. 2c), but not RD3 (Fig. 2b), antibody. In case #40 (exon 13, G389R), a few or a moderate number of pyramidal neurons with amorphous tau deposits were seen in AT8 stained sections, these sometimes having a rounded appearance resembling Pick bodies. Many thread-like structures were also seen within deeper layers of the frontal cortex. Occasionally, the Pick-like bodies were stained with RD3 antibody, but not with ET3.

In cases #40 and 41 (exon 13, R406W) many nerve cells containing diffuse cytoplasmic tau deposits or well-formed NFT were seen in AT8 immunostained sections (Fig. 2d). These NFT were strongly stained with RD3 (Fig. 2e), but less so with ET3 (Fig. 2f).

MAPT mutations in exon 10

A similar tau pathology was seen in the 8 cases with N279K *MAPT* mutation in exon 10 (patients #16-23), albeit these cases were from two different kindreds and

of different ethnic background (Japanese, cases #16 and 17 and North American/Caucasians, cases # 18-23). This was characterised in AT8 immunostained sections by the presence of pyramidal neurons in frontal cortex containing either amorphous cytoplasmic tau deposits or deposits resembling NFT (Fig. 3a), along with variable numbers of ballooned neurons and widespread glial cell tangles within grey matter and, especially within, white matter (Fig. 3d). These neuronal and glial cell tau deposits were strongly stained with ET3 (Fig. 3c, f) antibody, but not, or only rarely so in occasional cases, with RD3 antibody (Fig. 3b, e). The patient with *MAPT* N296H mutation (case #24) and those with *MAPT* exon 10 +16 splice site mutation (cases #30-35) showed similar changes to those with *MAPT* N279K mutation.

In the case with *MAPT* S305S mutation (case #29), a moderate number of small curvilinear, ring or crescent-shaped bodies were seen in neurons on AT8 staining. These were also stained with ET3 but not RD3 antibody. In cases with P301L mutation (cases #25-28), a moderate number of, or many, diffuse cytoplasmic and NFT-like tau aggregates were seen in pyramidal neurons on AT8 immunostaining, along with many neuropil threads (Fig. 3g). Many of the